

"This document is intended for publication in the open literature. It is made available on the understanding that it may not be further circulated and extracts may not be published prior to publication of the original, without the consent of the Publications Officer, JET Joint Undertaking, Abingdon, Oxon, OX14 3EA, UK".

"Enquiries about Copyright and reproduction should be addressed to the Publications Officer, JET Joint Undertaking, Abingdon, Oxon, OX14 3EA".

‘Helium and Neon Transport Experiments at JET’

M von Hellermann, K.Barth, A.J.Bickley, D.Campbell, U.Gerstel, J de Haas, D.Hillis*,
L.Horton, A.Howman, R.König, L.Lauro-Taroni, C.Mayaux, P.Nielsen, W.Obert, G.Saibene,
M.F.Stamp, D.Stork, M.Wade*, K-D Zastrow
JET Joint Undertaking, Abingdon, OX14 3EA, UK, *ORNL, Oak Ridge, Tennessee, USA

I. Introduction - In the pumped divertor phase of JET, dedicated helium transport experiments were carried out based on edge and central (beam) fuelling. Exhaust studies involve the use of argon frost on the divertor cryo-pump in order to achieve active pumping of helium. Charge exchange spectroscopy measurements are used to monitor the evolution of helium density profiles. Transport and exhaust of neon and nitrogen was investigated in radiative divertor experiments.

II. Helium Confinement and Exhaust Studies - The helium content added by the short (0.1s) gas-puffs is of the order 2 to $3 \cdot 10^{20}$ (or 5% of the total plasma particle content). Particle replacement times are experimentally determined by the measurement of the volume integrated impurity density profiles (He, Ne, N) and the temporal evolution of inward and

$$\tau_p^* = \frac{\int dV \cdot n_Z(\rho)}{A \cdot (\Gamma_{out} - \Gamma_{in})}$$

outward radial particle flows:

pulse	comment	P _{NB} MW	I _p MA	n _e (0) 10 ¹⁹ m ⁻³	n _α (0) 10 ¹⁸ m ⁻³	T _e (0) keV	Ar- frost	* τ _p (s)	τ _F (s)
33333	ELMy H-mode scan of x-point	10.5	2.0	5.0	2.1	5.0	yes	5-10	0.25
33476	L-mode	5.0	2.0	3.5	1.8	3.5	no	>11	0.24
33994	L-mode	13.0	2.0	3.5	4.2	4.0	yes	3.2±0.3	0.25
33995	ELMy H-mode	4.0	2.0	4.0	3.4	3.0	yes	>12	0.45
34324	ELMy H-mode	4.0	2.0	4.0	1.5	3.0	no	>22	0.64

Table I Overview of plasma data in representative helium edge puff experiments with active argon frost pumping (divertor target tiles are graphite).

Typical τ_p^* values for helium are of the order 8 to 15s (H-mode) in the case of active argon-frost pumping, compared to 20 to 30s in the case of no argon-frost (Fig.1). Corresponding values for L-mode confinement are approximately half the values of the H-mode case. The observed alpha particle replacement times exceed energy confinement times τ_E , which are of the order 0.3 to 0.5s, by more than a factor of 20 (H-mode, argon-frost) and 5 to 10 (L-mode, argon-frost). Time dependent variations of the particle replacement time following the initial pump phase indicate saturation effects in argon frost pumping. Sweeping of the x-point and the location of the strike zone with respect to the pump duct leads to significant changes in deduced particle decay rates (Fig.2). The L-mode evolution of N_{He}^{tot} (no active helium

pumping) (Fig. 1a) is described by a fast decrease (<30ms) following the initial peak induced by the gas puff and settling then to a steady level which is determined by the recycling level.

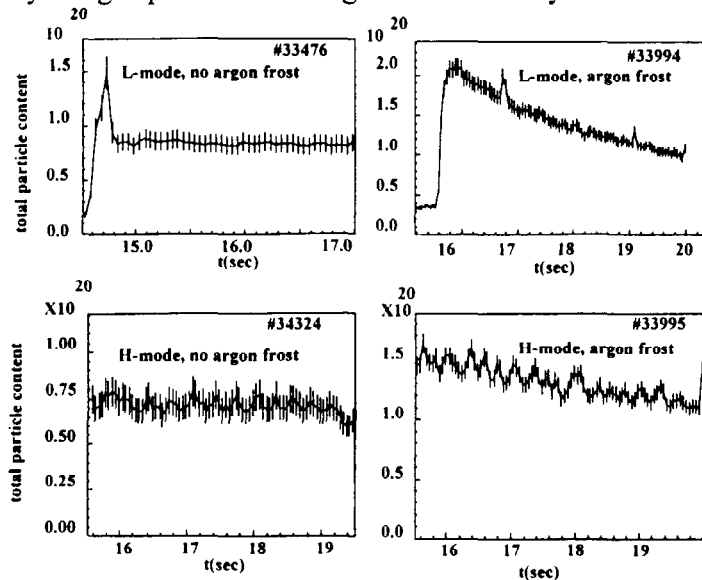


Fig.1 Decay of total alpha particle content in the case of no Ar-frost for a) H-mode, b) L-mode and active Ar frost pumping, c) H-mode d) L-mode.

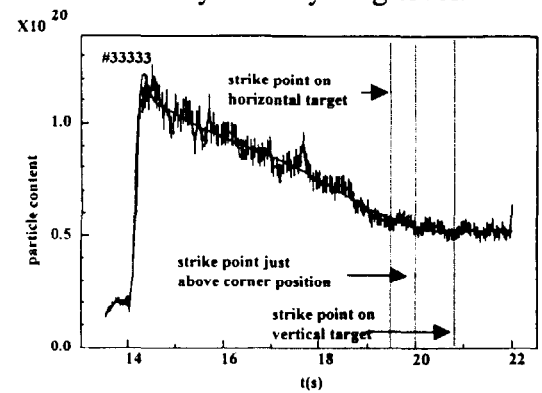


Fig.2 a) Particle content and variation of its decay rate in the case of sweeping of x-point and strike zone position. The decay rate reaches a maximum at a position close to the corner points of the divertor. Next to no pumping is observed when the strike zone is on the vertical target plates.

pulse	comment	P _{NBI} MW	I _p MA	n _e (0) 10 ¹⁹ m ⁻³	n _{Ne} (0) 10 ¹⁷ m ⁻³	T _e (0) keV	τ _p [*] (sec)	τ _E (sec)
32778	ELMy-H-mode	18.0	3.0	5.0	1.1	5.0	5.5	0.38
33958	L-mode	10.0	2.0	3.0	2.0	4.5	1.8±0.1	0.20
34372	L-mode	14.0	2.0	2.5	1.6	5.0	1.3±.07	0.26

Table II Overview of plasma data in neon edge fuelling and exhaust studies in L- and H-modes

III Neon exhaust in radiative divertor plasmas - Distinctively lower particle replacement times are observed in the case of neon gas-puff experiments (see table II), which were carried out as part of divertor radiative cooling studies. Similar to helium the H-mode particle confinement time τ_p^* is about 2 to 3 times the L-mode case. Fig.3 shows the rapid decay of the Ne¹⁰⁺ content following a puff of 200ms. Neon particle replacement times are about 5 to 10 times the energy confinement time.

IV. Experimental transport data (He gas-puff experiments) - Substantial progress has been achieved in the last experimental campaign at JET by a simultaneous measurement of carbon and helium CX spectra. By imposing the ion temperature deduced from CX CVI the uncertainties in the analysis of the HeII spectrum - in particular in erroneous profiles gradients induced by 'plume' effects etc. - can be much reduced. Diffusion coefficients and convective velocities are derived from particle flows Γ_z and gradients ∇n_z (i.e. $\frac{\Gamma_z}{n_z} = -D \frac{\nabla n_z}{n_z} + v_z$) measured during the period of density perturbation following the brief edge gas puff.

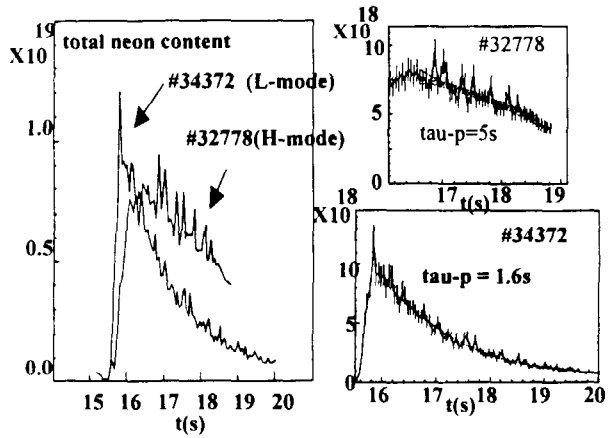


Fig.3 Total confined neon content and its decay in L-mode and H-mode

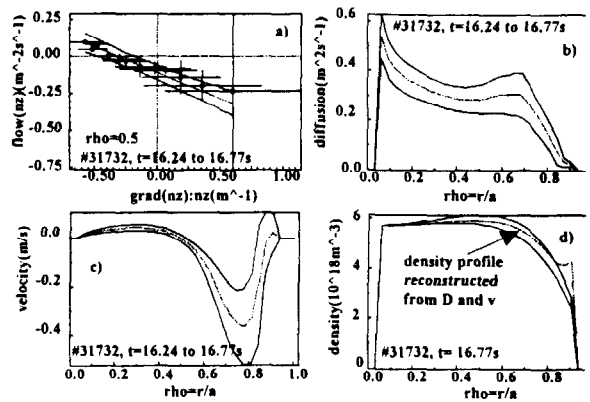


Fig.4a) Deduction of transport data from $\Gamma(nz)/nz$ and $\nabla(nz)/nz$, b) $D(\rho)$, c) $v(\rho)$, d) steady state reconstruction of density profiles from $v(r)$, $D(r)$ and comparison with experimental upper and lower error bars.

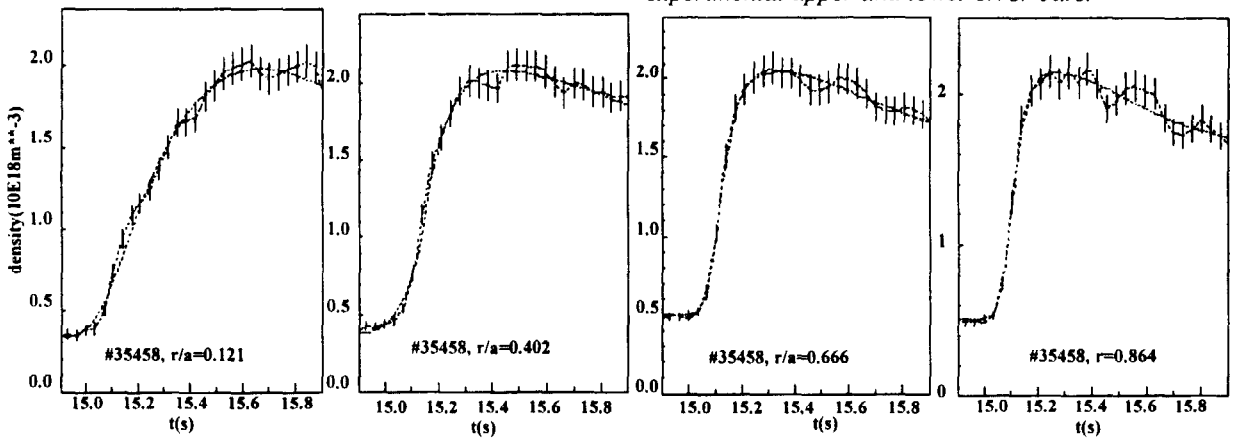


Fig.5 Helium profile evolution during an H-mode, radiative divertor, gas-puff experiment (Be target tiles) Experimental data and spline fit shown for 4 minor radii. Vertical bars indicate statistical errors.

B) Neon transport studies - Neon density profiles (similar to the intrinsic impurity carbon) remain even during substantial edge fuelling hollow (both in L- and H-mode) and convection velocities are directed outwards for the major part of the profiles.

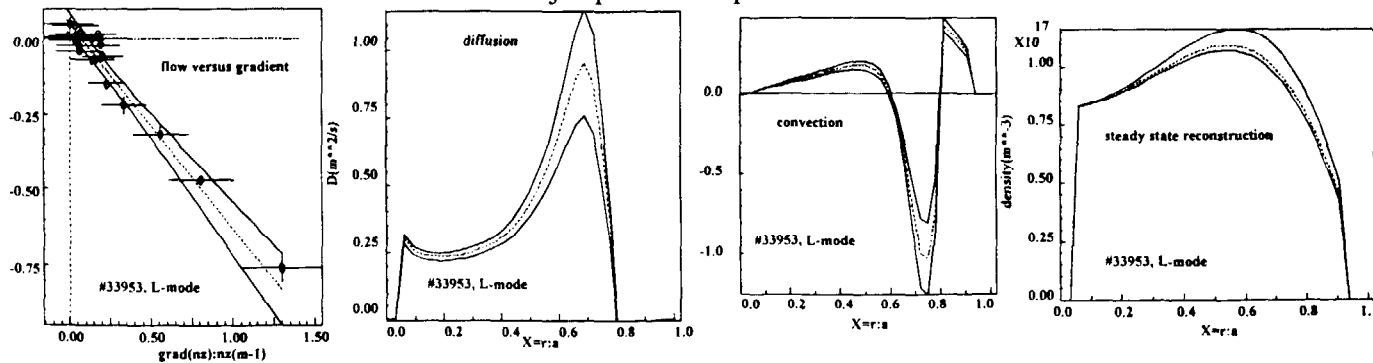


Fig.6 Deduction of neon transport data in L-mode confinement phase.

V. Beam fuelling experiments - A few experiments were performed with H- and L-mode helium core fuelling making use of the two neutral beam boxes at JET one acting as a source of high energy neutral helium and the second as diagnostic beam.

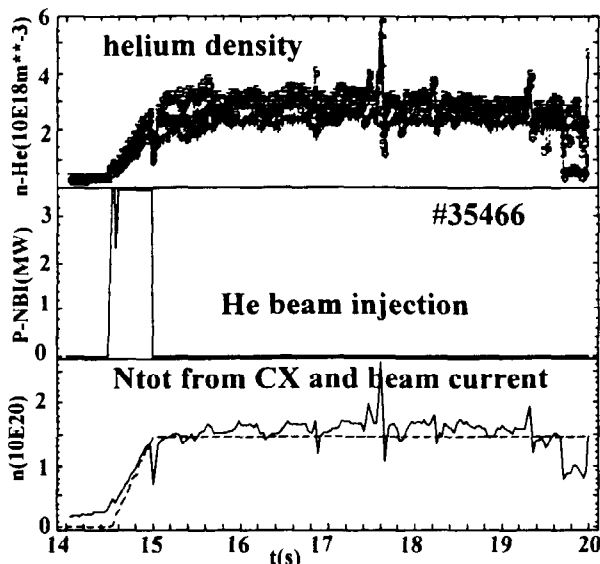


Fig.7 H-mode case, #35466, time traces of helium density, NBI power and particle content.

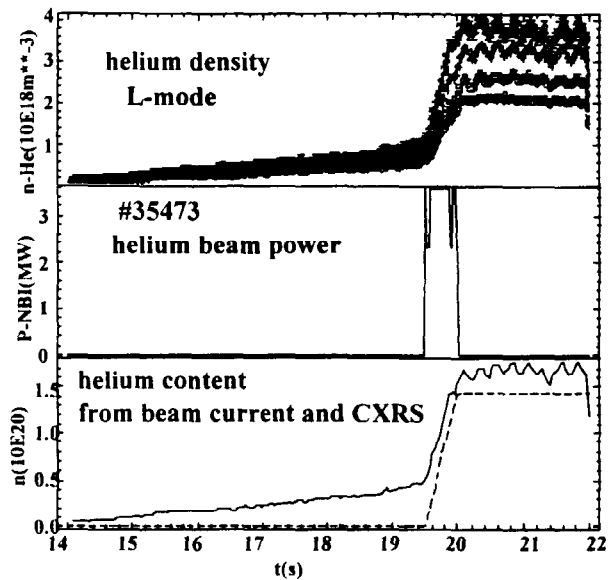


Fig.8 L-mode case, #35473, time traces of helium density, NBI power and particle content.

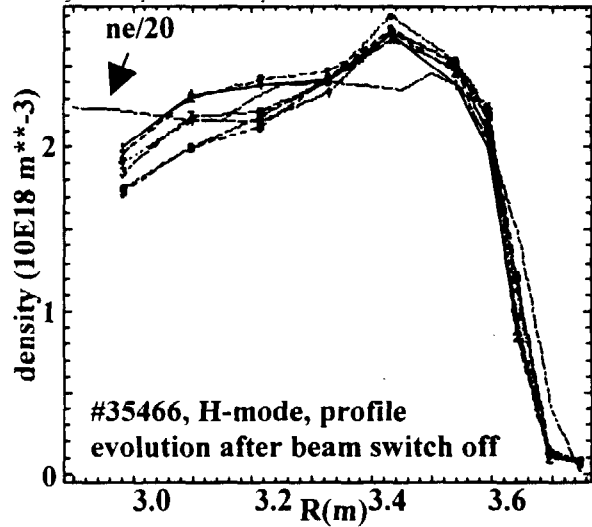
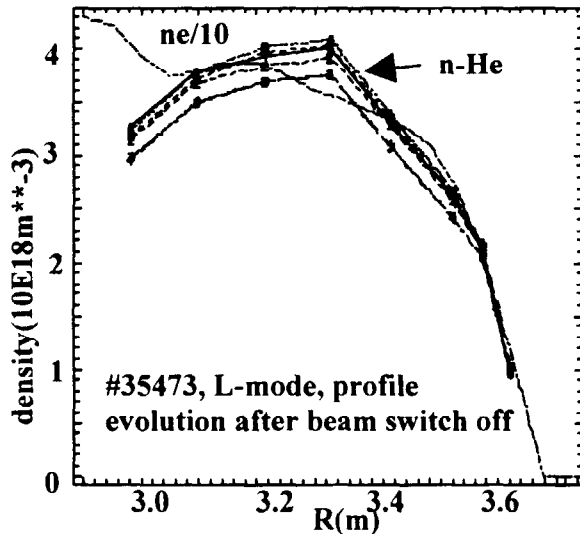


Fig.9 Profile evolution after switching-off the He fuelling beam a) L-mode #35473, b) H-mode #35466. For comparison electron density profile (divided by 10 and 20 respectively). Profiles at 20.1s and every 35ms.

Conclusion - Edge and central fuelling experiments were performed in the JET divertor phase. Active pumping was achieved by deposition of an argon frost layer on the divertor cryo-pumps. The observed helium replacement times $\tau_p^* \gg \tau_E$ indicate that the development of efficient helium pumps will have to play a key role on the route to acceptable values of τ_p^* . Edge and core fuelling have demonstrated that steady state helium profiles are reached on a short time scale (both in H- and L-mode), and that in contrast to intrinsic impurity profiles, such as Be, Ne, or C, which are found to be consistently hollow, helium assumes profile shapes very similar to that of electron density profiles. No evidence at all is found of either helium accumulation on the magnetic axis or close to the separatrix. Core transport appears therefore not to be a limiting factor for projected next-step devices.